Acta Crystallographica Section B
Structural Science
ISSN 0108-7681

Powder diffraction crystal structure analysis using derivative difference minimization: example of the potassium salt of 1-(tetrazol-5-yl)-2-nitroguanidine

Leonid A. Solovyov,[a]* A. M. Astachov,[b] M. S. Molokeev[c] and A. D. Vasiliev[c]

[a]Institute of Chemistry and Chemical Technology, 660049 Krasnoyarsk, Russia, [b]Siberian State Technological University, 660049 Krasnoyarsk, Russia, and [c]Kirensky Institute of Physics, 660036 Krasnoyarsk, Russia

Correspondence e-mail: leosol@icct.ru

Received 27 March 2005
Accepted 10 May 2005

The crystal structure of the potassium salt of 1-(tetrazol-5-yl)-2-nitroguanidine [$K(C_2H_3N_8O_2)$] was solved and refined from X-ray powder diffraction data by applying the derivative difference minimization (DDM) method. The compound is of interest as an energetic substance. The structure model was found from a Patterson search. The reflection intensities for the Patterson synthesis were derived from the powder profile by applying a newly developed DDM-based profile decomposition procedure. The use of the DDM method allowed successful location and unconstrained refinement of all the atomic positions, including those of three independent H atoms. The advantages of DDM in terms of the precision and reproducibility of the structural parameters are discussed in comparison to Rietveld refinement results. The failure to refine the H-atom positions by the Rietveld method was attributed to systematic errors associated with the background modelling, which are avoided by DDM.

1. Introduction

The precision of crystal structure analysis by powder diffraction as well as the complexity of the structures studied have grown with the development of modern equipment and methods. However, the quality of structural data obtained by powder diffraction is, generally, far from that normally achieved in single-crystal studies. In particular, the location and unconstrained refinement of H-atom positions from X-ray powder diffraction data have so far been successful in only a few exceptional cases (*e.g.* Cernik *et al.*, 1991; Schwartz & Von Dreele, 1997; Schmidt *et al.*, 1998; Dinnebier *et al.*, 1999; Leineweber *et al.*, 1999; Soulie *et al.*, 2002). The most obvious reason is the peak overlap which reduces the amount of information contained in the diffraction pattern. Furthermore, the peak overlap induces another serious problem, which is the ambiguity of the background scattering curve. In Rietveld's (1969) method this problem is approached by using various analytical approximations of the background, such as polynomial or Fourier series *etc.* However, these approximations do not provide a correct modelling of the background curve which is universally applicable. A general solution of this problem has been recently proposed using the derivative difference minimization (DDM) method (Solovyov, 2004). In this method the refinement is aimed not at minimizing the absolute difference between the observed and calculated profiles, but at minimizing the oscillations (or curvature) of the difference curve. The squared values of the difference curve derivatives are used in DDM as a measure of the difference curvature. The main advantage of this method is that it does not involve background-line modelling or approximations,

Table 1
Experimental details.

Crystal data	
Chemical formula	$C_2H_3KN_8O_2$
M_r	210.20
Cell setting, space group	Triclinic, $P\bar{1}$
a, b, c (Å)	7.0310 (1), 11.4089 (1), 4.6788 (1)
α, β, γ (°)	93.158 (1), 106.749 (1), 83.473 (1)
V (Å^3)	356.96 (1)
Z	2
D_x (Mg m^{-3})	1.956
Radiation type	Cu $K\alpha$
Temperature (K)	293
Specimen form, colour	Powder, colourless
Specimen size (mm)	20 × 20 × 0.5
Data collection	
Diffractometer	DRON-4
Data collection method	Specimen mounting: packed powder pellets; mode: reflection; scan method: step
2θ (°)	$2\theta_{min}$ = 7, $2\theta_{max}$ = 107, increment = 0.02
Refinement	
Refinement on	I_{net}
R factors	R_{DDM} = 0.072, R_B = 0.032
Wavelength of incident radiation (Å)	1.5418
Excluded region(s)	None
Profile function	Pearson VII
No. of parameters	89
H-atom treatment	Only coordinates refined
Weighting scheme	Based on measured s.u.'s
$(\Delta/\sigma)_{max}$	<0.0001

Computer programs used: DDM (Solovyov, 2004).

thus avoiding systematic errors caused by inadequate background definitions.

The first applications of DDM in the structural studies of crystalline (Solovyov, 2004; Jacob *et al.*, 2005) and mesostructured materials (Solovyov *et al.*, 2005; Kleitz *et al.*, 2004; Kim *et al.*, 2005) have demonstrated its capabilities for obtaining precise structure characteristics from diffraction data with different background complexities. In the present work the DDM method is used for crystal structure determination and refinement of the potassium salt of 1-(tetrazol-5-yl)-2-nitroguanidine (TetrNQ). TetrNQ is of interest as an energetic compound (Astachov *et al.*, 2001; Astachov, Sokolenko *et al.*, 2002; Astachov, Gelemurzina *et al.*, 2003). Its molecular structure and, in particular, the location of the H atoms studied as a sample suitable for single-crystal XRD analysis could not be obtained. Quantum-chemical calculations, both semi-empirical and *ab initio*, produced the most energetically favorable configuration with the iminotetrazole radical conformation, as shown in (I*b*), which is opposite to the classical tetrazole fragment structure (I*a*) (Astachov *et al.*, 2001; Astachov, Sokolenko *et al.*, 2002). Both structures (I*a*) and (I*b*) contain similar molecular fragments and, therefore, elemental analysis, UV and FTIR spectroscopic data could not distinguish between them. ^{1}H, ^{13}C and ^{15}N NMR spectroscopy studies of TetrNQ in solution (Astachov, Sokolenko *et al.*, 2002) did not assign the correct structural type. Owing to the possibility of fast proton exchange, the observed NMR spectra could be equally explained by both conformations.

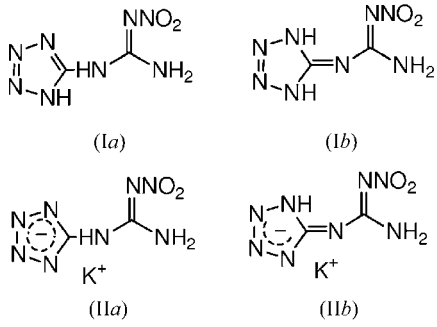

There was a similar ambiguity in the structure of the potassium salt of TetrNQ. While suitable single crystals of the salt were also not available, the product was synthesized as a single-phase polycrystalline powder (Astachov *et al.*, 2001; Vasiliev *et al.*, 2001).

Here we present the results of a comprehensive analysis of the potassium tetrazol-nitroguanidine crystal structure from powder XRD data using the DDM method. All the atomic positions, including those of the H atoms, were successfully determined and refined by applying the DDM method without restraints. A DDM-based profile decomposition procedure was proposed and its application in the structure determination was demonstrated. The reproducibility and precision of the results obtained by both DDM and Rietveld methods were comparatively analyzed and discussed.

2. Experimental

2.1. Materials and measurements

The synthesis of the potassium salt of TetrNQ has been described elsewhere (Astachov *et al.*, 2001; Astachov, Gelemurzina *et al.*, 2003). The samples for the powder XRD measurements were prepared by applying two different techniques. Sample *A* was a densely packed crystalline powder in a quartz holder. The excess powder was cut by a sharp razor to reduce the surface texture, while the preferred orientation in the bulk sample could not be avoided. Sample *B* was prepared by dusting the finely ground material powder on a silicon zero-background holder surface covered by an adhesive. This technique normally minimizes the preferred orientation effect, which often interferes with structure solution and refinement purposes. On the other hand, densely packed samples provide a better signal-to-noise ratio and peak resolution, especially for the high-angle region of a powder pattern. The reason why both samples were used for the structure analysis was to check the reproducibility of the results.

XRD data were collected on a laboratory powder diffractometer (DRON-4, Cu $K\alpha$ radiation) equipped with a secondary flat graphite monochromator. The measurements were performed from Bragg–Brentano geometry at room

temperature. The experimental details are summarized in Table 1.

2.2. Computational details

The triclinic unit-cell parameters (Table 1) were obtained by indexing the powder pattern using the *ITO* program (Visser, 1969). The powder profile and structure refinement were performed using the DDM program (Solovyov, 2004), which is based on a modified version of *DBWS*-9006*PC* (Wiles & Young, 1981).

The XRD reflection intensities were extracted from the powder profile by applying an iterative DDM-based decomposition procedure. The procedure consisted of finding additions to the calculated (or initially set) reflection intensities for minimizing the squared angular derivatives of the difference diffraction profile. The calculated profile intensity Y_{ci} in the ith profile point is defined as

$$Y_{ci} = \sum_n I_{cn} f_n(\theta_i), \tag{1}$$

where I_{cn} is the calculated intensity of the nth reflection, $f(\theta)$ is the peak-shape function, θ is the diffraction angle and the sum is over the whole set of reflections contributing to the profile point. In accordance with the DDM methodology, the minimization function for an individual reflection can be written as

$$MF = \sum_i \left\{ w_i^1 \left[\frac{\partial}{\partial\theta} \left(\Delta_i - f(\theta_i)\delta \right) \right]^2 + w_i^2 \left[\frac{\partial^2}{\partial\theta^2} \left(\Delta_i - f(\theta_i)\delta \right) \right]^2 + \ldots + w_i^k \left[\frac{\partial^k}{\partial\theta^k} \left(\Delta_i - f(\theta_i)\delta \right) \right]^2 \right\},$$
$$\Delta_i = Y_{oi} - Y_{ci}, \tag{2}$$

where Y_o is the observed profile intensity, w is the weight, δ is the addition to the reflection intensity and the sum is over the profile area to which the reflection contributes. Restricting the derivatives in MF to first and second order and minimizing with respect to δ gives

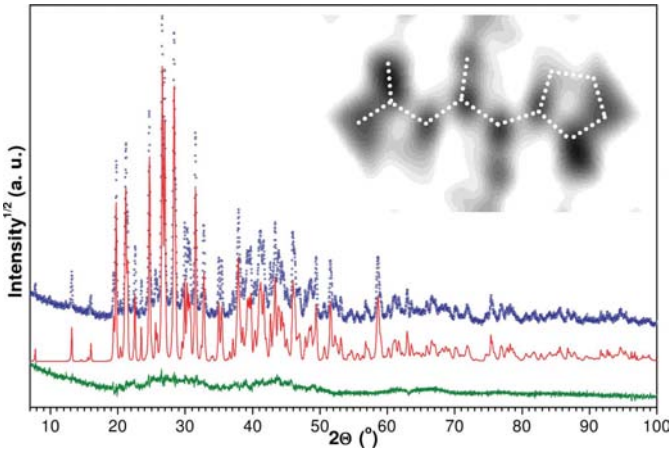

Figure 1
Weighted observed, calculated and difference XRD powder profiles for sample *A* after DDM decomposition. The insert shows a Patterson map section with the superimposed sketch of the TetrNQ anion.

$$\frac{\partial}{\partial\delta} MF = -2 \sum_i \left\{ w_i^1 \delta \frac{\partial}{\partial\theta} f(\theta_i) \frac{\partial}{\partial\theta} \left(\Delta_i - f(\theta_i)\delta \right) + w_i^2 \delta \frac{\partial^2}{\partial\theta^2} f(\theta_i) \frac{\partial^2}{\partial\theta^2} \left(\Delta_i - f(\theta_i)\delta \right) \right\} = 0 \tag{3}$$

from which

$$\delta = \frac{\sum_i \left\{ w_i^1 \frac{\partial}{\partial\theta} f(\theta_i) \frac{\partial}{\partial\theta} \Delta_i + w_i^2 \delta \frac{\partial^2}{\partial\theta^2} f(\theta_i) \frac{\partial^2}{\partial\theta^2} \Delta_i \right\}}{\sum_i \left\{ w_i^1 \left[\frac{\partial}{\partial\theta} f(\theta_i) \right]^2 + w_i^2 \left[\frac{\partial^2}{\partial\theta^2} f(\theta_i) \right]^2 \right\}}. \tag{4}$$

Applying the Savitzky–Golay formalism (Savitzky & Golay, 1964) for the derivative calculation we may rewrite (4) as

$$\delta = \frac{\sum_i \left\{ w_i^1 \sum_{j=-m}^{m} c_j^1 f(\theta_{i+j}) \sum_{j=-m}^{m} c_j^1 \Delta_{i+j} + w_i^2 \sum_{j=-m}^{m} c_j^2 f(\theta_{i+j}) \sum_{j=-m}^{m} c_j^2 \Delta_{i+j} \right\}}{\sum_i \left\{ w_i^1 \left[\sum_{j=-m}^{m} c_j^1 f(\theta_{i+j}) \right]^2 + w_i^2 \left[\sum_{j=-m}^{m} c_j^2 f(\theta_{i+j}) \right]^2 \right\}} \tag{5}$$

$$w_i^k = \left[\sum_{j=-m}^{m} (c_j^k)^2 (\sigma_{i+j})^2 \right]^{-1}, \tag{6}$$

where c_j^k are the Savitzky–Golay coefficients for the derivative of the order k with the profile convolution interval $[-m, m]$ and σ_i is the variance in the experimental profile intensity Y_{oi}. Considering the peak overlap, because of which several reflections may contribute to the same profile area, the addition δ should be reduced by an appropriate overlap correction. Finally, the estimated 'observed' reflection intensity is given by

$$I_{\rm obs} = I_c + \delta \frac{f(\theta^0) I_c}{Y_c^0}, \tag{7}$$

$$Y_c^0 = \sum_n I_{cn} f_n(\theta^0), \tag{8}$$

where θ^0 is the reflection position, $f(\theta^0)$ and Y_c^0 are the values of the peak-shape function and the calculated profile intensity in the position θ^0; δ is obtained from (5). The multiplier after δ in (7) represents the overlap correction factor.

The result of the application of the DDM decomposition formula (7) is similar to that of Rietveld's approximation for $I_{\rm obs}$ (Rietveld, 1969), except that it is DDM-oriented and thus does not require a background definition. In the DDM program (7) is also used for the Bragg R-factor calculation. For single non-overlapped peaks or a set of peaks with the same position, the DDM decomposition formula immediately gives the best estimate for $I_{\rm obs}$. For partly overlapped peaks it should be iterated to arrive at an optimized set of $I_{\rm obs}$ similarly to the Le Bail method (Le Bail *et al.*, 1988). The starting intensities I_c can either be calculated from an existing structure model or set arbitrarily when the model is absent. It should be noted that for fully overlapped peaks the DDM decomposition procedure automatically preserves the initial set ratio of intensities, which is important when estimated

values of I_{obs} are used in the difference Fourier map calculations.

2.3. Structure determination and refinement

The structure model of the potassium salt of TetrNQ was obtained from a Patterson map analysis, which located all the non-H atoms. The reflection intensities for the Patterson synthesis were derived from the powder profile by applying the DDM decomposition procedure. Fig. 1 shows the consistency between the observed and calculated XRD profiles after the DDM decomposition and a section of the Patterson map with the superimposed molecule sketch. A Patterson map generated from the intensities extracted by the Le Bail method allowed analogous interpretation of the main structure fragment.

The structure was refined by the DDM method using XRD data from sample *A*. The Pearson VII peak-shape function was applied. The anisotropic peak broadening due to microstrain was modelled by the ellipsoidal approximation

$$\mathrm{FWHM}^2 = (S_1h^2 + S_2k^2 + S_3l^2 + S_4 2hk + S_5 2hl + S_6 2kl)d^2 \tan^2\theta + V\tan\theta + W, \quad (9)$$

where FWHM is the peak full width at half-maximum, d is the d spacing, hkl are the reflection indexes, and S_1–S_6, V and W are adjustable parameters. The preferred orientation correction was applied in the form

$$\mathrm{PREF} = [1 + (P_1h^2 + P_2k^2 + P_3l^2 + P_4 2hk + P_5 2hl + P_6 2kl)d^2/100]^{-3/2}, \quad (10)$$

where P_1– P_6 are adjustable parameters. During the Rietveld refinement the background was modelled by a fifth-degree polynomial with six adjustable parameters.

During the first stages of the refinement the geometrically determined H-atom positions of the imino group were added to the structure model and firmly attached to the respective N atom. The remaining hydrogen position was located on the difference E map based on the I_{obs} intensities derived from the XRD pattern of sample *A* by the DDM decomposition procedure. Figs. 2(*a*) and (*b*) show the direct and difference E-map sections. While the difference map is rather noisy, it clearly shows maximal peaks near the N-atom positions. Finally, all the profile and structural parameters, including the positions of the H atoms, were refined by the DDM method without restraints. The final DDM plot and the conformation of the anion obtained by the refinement are shown in Fig. 3. The difference map after complete structure refinement (Fig. 2*c*) did not reveal any additional interpretable features.

In the DDM refinement for sample *B* as well as in the Rietveld refinement for both samples *A* and *B*, the H atoms were constrained to be attached to the N atoms, without which it was impossible to attain an acceptable molecular geometry. To verify the location of the H3 atom, an additional hydrogen position (H4) was included in the structure model and attached

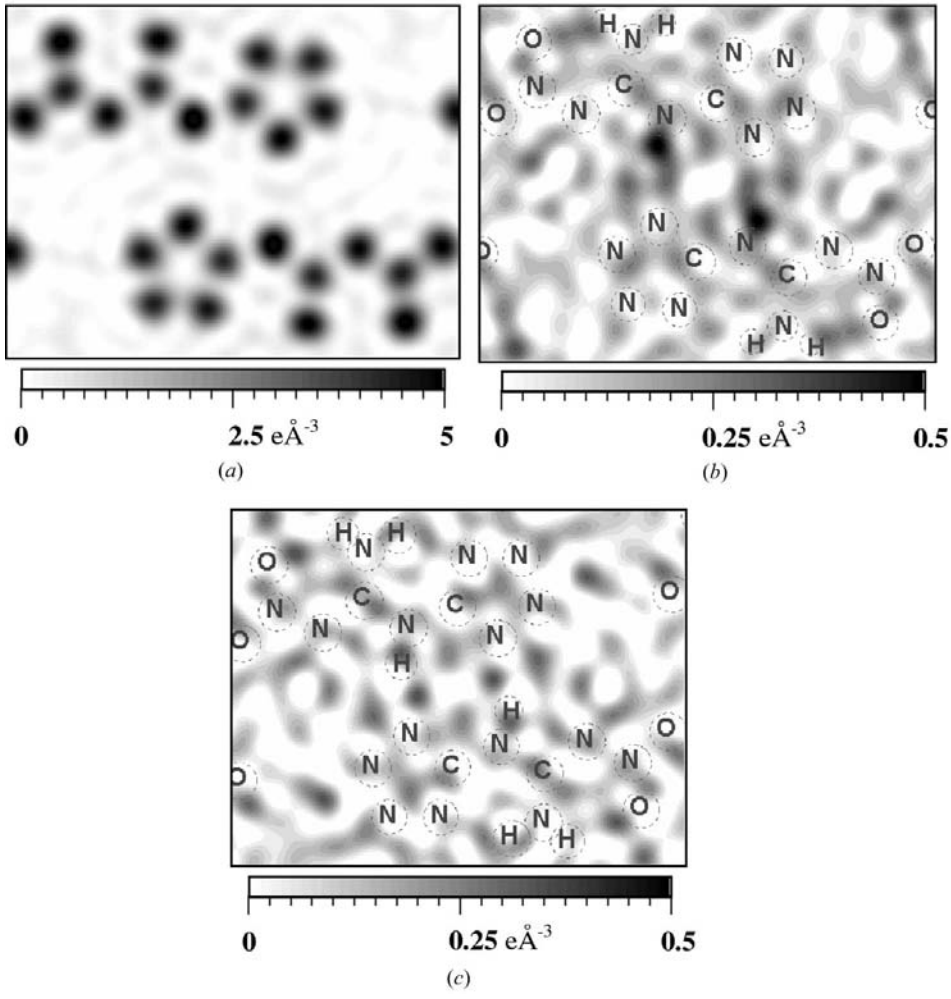

Figure 2
(*a*) Sections of the E map, (*b*) the difference map without the H3 atom and (*c*) after DDM refinement of the complete structure, including all H atoms.

Table 2
Selected geometric parameters (Å, °) and their differences (Δ) obtained from DDM and Rietveld refinement for samples *A* and *B*.

	Sample *A*	Sample *B*	Δ		Sample *A*	Sample *B*	Δ
DDM refinement							
K···O1^{i}	2.886 (4)	2.897 (6)	−0.011	O1—N1—N2	124.5 (5)	124.1 (7)	0.4
K···O1^{ii}	2.838 (4)	2.826 (6)	0.012	O2—N1—N2	114.1 (4)	116.2 (7)	−2.1
K···O2^{iii}	2.949 (4)	2.947 (5)	0.002	O1—N1—O2	121.4 (5)	119.4 (7)	2.0
K···O2^{iv}	2.754 (5)	2.775 (6)	−0.021	N1—N2—C1	118.2 (4)	119.2 (7)	−1.0
K···O2^{i}	2.962 (5)	2.943 (6)	0.019	N2—C1—N3	128.7 (6)	126.3 (7)	2.4
K···N2^{iii}	2.895 (5)	2.902 (6)	−0.007	N2—C1—N4	111.0 (5)	108.3 (7)	2.7
K···N6	2.893 (6)	2.919 (9)	−0.026	N3—C1—N4	120.3 (7)	125.4 (8)	−5.1
K···N7^{v}	2.829 (5)	2.853 (9)	−0.024	C1—N4—C2	125.4 (5)	123.0 (7)	2.4
N1—O1	1.255 (6)	1.281 (9)	−0.026	N4—C2—N5	126.0 (6)	123.4 (7)	2.6
N1—O2	1.263 (6)	1.268 (9)	−0.005	N4—C2—N8	119.6 (5)	123.1 (7)	−3.5
N1—N2	1.320 (6)	1.319 (10)	0.001	N5—C2—N8	114.4 (7)	113.5 (8)	0.9
N2—C1	1.385 (7)	1.397 (10)	−0.012	C2—N8—N7	103.5 (4)	104.1 (7)	−0.6
C1—N3	1.279 (11)	1.291 (11)	−0.012	N8—N7—N6	110.9 (4)	110.3 (8)	0.6
C1—N4	1.362 (8)	1.319 (10)	0.043	N5—N6—N7	108.4 (4)	109.6 (7)	−1.2
N4—C2	1.401 (8)	1.421 (11)	−0.020	C2—N5—N6	102.8 (4)	102.5 (7)	0.3
C2—N5	1.347 (9)	1.338 (11)	0.009	C1—N3—H1	126 (3)		
N5—N6	1.364 (7)	1.372 (11)	−0.008	C1—N3—H2	120 (3)		
N6—N7	1.353 (6)	1.317 (11)	0.036	H1—N3—H2	108 (4)		
N7—N8	1.326 (6)	1.327 (10)	−0.001	C1—N4—H3	109 (2)		
N8—C2	1.338 (8)	1.340 (11)	−0.002	C2—N4—H3	124 (2)		
N3—H1	0.83 (5)						
N3—H2	0.97 (5)						
N4—H3	0.99 (4)						
Rietveld refinement†							
K···O1^{i}	2.898 (5)	2.891 (9)	0.007	O1—N1—N2	126.0 (7)	121.8 (10)	4.2
K···O1^{ii}	2.838 (6)	2.853 (8)	−0.015	O2—N1—N2	118.1 (6)	128.3 (10)	−10.2
K···O2^{iii}	2.974 (5)	2.970 (9)	0.004	O1—N1—O2	115.8 (7)	109.4 (9)	6.4
K···O2^{iv}	2.766 (5)	2.806 (11)	−0.040	N1—N2—C1	115.4 (5)	122.2 (10)	−6.8
K···O2^{i}	2.925 (5)	2.913 (10)	0.012	N2—C1—N3	132.3 (7)	127.5 (10)	4.8
K···N2^{iii}	2.880 (6)	2.967 (13)	−0.087	N2—C1—N4	106.4 (5)	103.2 (10)	3.2
K···N6	2.888 (7)	2.910 (14)	−0.022	N3—C1—N4	121.2 (7)	127.5 (15)	−6.3
K···N7^{v}	2.833 (8)	2.890 (14)	−0.057	C1—N4—C2	126.5 (5)	120.1 (10)	6.4
N1—O1	1.290 (9)	1.360 (12)	−0.070	N4—C2—N5	123.6 (6)	126.8 (10)	−3.2
N1—O2	1.273 (8)	1.253 (14)	0.020	N4—C2—N8	125.5 (6)	121.9 (10)	3.6
N1—N2	1.306 (8)	1.250 (16)	0.056	N5—C2—N8	110.9 (7)	111.2 (10)	−0.3
N2—C1	1.405 (9)	1.399 (18)	0.006	C2—N8—N7	106.0 (5)	103.5 (10)	2.5
C1—N3	1.246 (9)	1.227 (18)	0.019	N6—N7—N8	110.5 (6)	112.7 (10)	−2.2
C1—N4	1.375 (9)	1.326 (17)	0.049	N5—N6—N7	109.9 (5)	108.3 (10)	1.6
N4—C2	1.363 (8)	1.425 (16)	−0.062	C2—N5—N6	102.5 (5)	103.1 (9)	−0.6
C2—N5	1.405 (9)	1.375 (18)	0.030				
N5—N6	1.385 (8)	1.357 (16)	0.028				
N6—N7	1.335 (9)	1.317 (16)	0.018				
N7—N8	1.331 (8)	1.300 (16)	0.031				
N8—C2	1.357 (9)	1.366 (17)	−0.009				

Symmetry codes: (i) $x, y-1, z$; (ii) $-x, 1-y, -z$; (iii) $1-x, 1-y, 1-z$; (iv) $x, y-1, 1+z$; (v) $x, y, 1+z$. † Geometric parameters for H atoms are not listed since their positions were not refined.

to the N8 atom. The DDM and Rietveld refinements for both samples *A* and *B* were repeated with varying occupancies of the atomic positions H3 and H4. In all cases the occupancy of H3 was close to 100% and the occupancy of H4 was around zero.

3. Results and discussion

The final structural parameters obtained by DDM and Rietveld refinement for samples *A* and *B* are summarized in Tables 2 and 3.[1] Comparing the parameters it becomes apparent that the reproducibility of the DDM results for samples *A* and *B* is much higher than in the case of Rietveld refinement. The overall mean difference in the interatomic distances determined for samples *A* and *B* is *ca* 0.016 Å for DDM and *ca* 0.032 Å for Rietveld refinement. The molecular geometry from Rietveld refinement for sample *A* is slightly worse than that from DDM with respect to the geometry of similar fragments known from single-crystal studies (see the discussion below). For sample *B* the structural parameters obtained by Rietveld refinement are much worse (N1—N2, C1—N3, N—O distances, some angles, non-positive definite displacement parameters *etc.*).

The final DDM and Rietveld plots for samples *A* and *B* are shown in Figs. 3 and 4. In the DDM plots several broad background maxima can be clearly seen, two of them (between 60 and 80° 2θ in Fig. 4*a*) being due to scattering from the sample holder. Apparently, such a complex background cannot be adequately modelled by the polynomial function used in the Rietveld refinement, which allows for the advantageous DDM application. Taking into account the above considerations and, especially, the successful refinement of H-atom positions, we have chosen the results obtained by DDM for sample *A* as the best final structure solution.

The structure of the nitrimine molecular fragment of the potassium salt of TetrNQ determined in this study shows a close similarity with the structures of other nitroguanidines (Nordenson, 1981; Nordenson & Hvoslev, 1981; Rice *et al.*, 1984; Oyumi *et al.*, 1987; Bracuti, 1999; Astachov, Vasiliev *et al.*, 2002; Astachov, Vasiliev *et al.*, 2003; Vasiliev *et al.*, 2003*a*,*b*; Vasiliev, Astachov, Molokeev, Kruglyakova & Stepanov, 2004; Allen, 2002). The anion conformation is planar. The planar geometry is stabilized by two intramolecular hydrogen bonds, N3–H1···O1 and N3–H2···N5. Deviations from the least-squares plane through the non-H atoms are 0.028 (6) (r.m.s) and 0.112 (8) Å. The C—N, N—N and N—O bond lengths are intermediate between the values characteristic for the corresponding single and double bonds because of the delocalization of π electron density. The geometry of the nitro group is similar to that observed in other derivatives of nitroguanidine (Allen, 2002). The range of N—O distances in various nitroguanidine derivatives is relatively broad due to the different involvement of O atoms in the intra- and intermolecular bonds. In the potassium salt of TetrNQ, these distances are at

[1] Supplementary data for this paper are available from the IUCr electronic archives (Reference: SN5019). Services for accessing these data are described at the back of the journal.

Table 3
Hydrogen-bonding geometry (Å, °).

D—H···A	D—H	H···A	D···A	D—H···A
N3—H1···O1	0.83 (5)	2.13 (5)	2.576 (5)	114 (4)
N3—H2···N5	0.97 (5)	1.98 (5)	2.724 (6)	132 (4)
N4—H3···N8^{i}	0.99 (4)	1.97 (5)	2.861 (6)	149 (4)

Symmetry codes: (i) $1-x, 1-y, 2-z$.

the top limit of those observed for other nitroguanidine compounds owing to the involvement of the O atoms in the coordination of the potassium cation (Fig. 5). The N—O bond lengths determined correspond well with those in 5-nitraminotetrazole salts where the coordination of O atoms to cations takes place (Vasiliev, Astakhov, Nefedov *et al.*, 2003; Vasiliev, Astachov, Molokeev, Kruglyakova, Sirotinin & Stepanov, 2004; Astachov, Vasiliev, Molokeev, Kruglyakova, Sirotinin & Stepanov, 2004; Astachov, Vasiliev, Molokeev, Sirotinin, Kruglyakova & Stepanov, 2004). The angles O1—N1—N2, O2—N1—N2 and O1—N1—O2 correspond to those determined from single-crystal studies for other nitroguanidines, which are within the limits of 123–126, 115–117 and 117–121°, respectively. The C1—N3 bond length [1.279 (11) Å] is shorter than that in nitroguanidine and its derivatives (1.30–1.32 Å; Vasiliev *et al.*, 2003*a*,*b*; Vasiliev, Astachov, Molokeev, Kruglyakova & Stepanov, 2004; Astachov, Vasiliev *et al.*, 2002; Nordenson, 1981; Bracuti, 1999). While the bond length reduction is within several standard uncertainties, it was reproduced in all the refinement runs for both samples and can be explained by the influence of the two intramolecular hydrogen bonds. The angles N2—C1—N3 [128.7 (6)°], N3—C1—N4 [120.3 (7)°] and N2—C1—N4 [111.0 (5)°] are in fair agreement with their respective angles (126–130, 119–121 and 107–113°) in the above-mentioned known nitroguanidines.

The geometry of the tetrazole cycle is also similar to that observed in other compounds (Allen, 2002). The N—C—N and N—N—N angles observed exceed the C—N—N angles by around 10°, which is typical of most known tetrazole derivatives. The bond lengths C—N and N—N are essentially equal, which is typical for tetrazole salts compared with the parent tetrazoles. The increased C2—N4 bond length [1.401 (8) Å] indicates the absence of π–π electronic interactions between

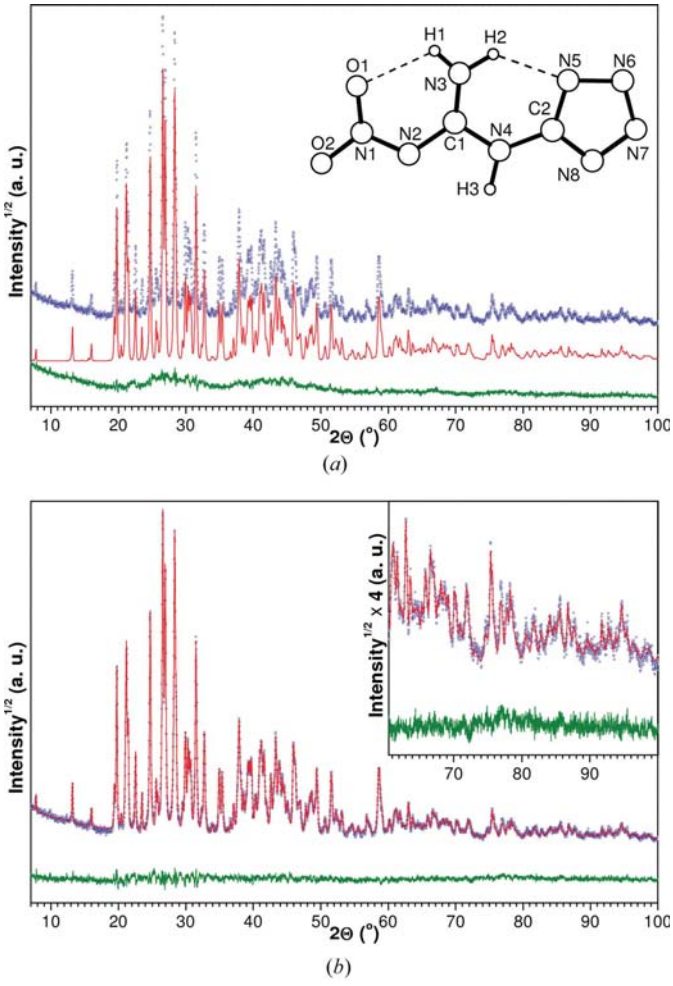

Figure 3
Weighted observed, calculated and difference XRD powder profiles for sample *A* after (*a*) DDM and (*b*) Rietveld refinement. The insert in (*a*) shows the molecular conformation obtained by DDM.

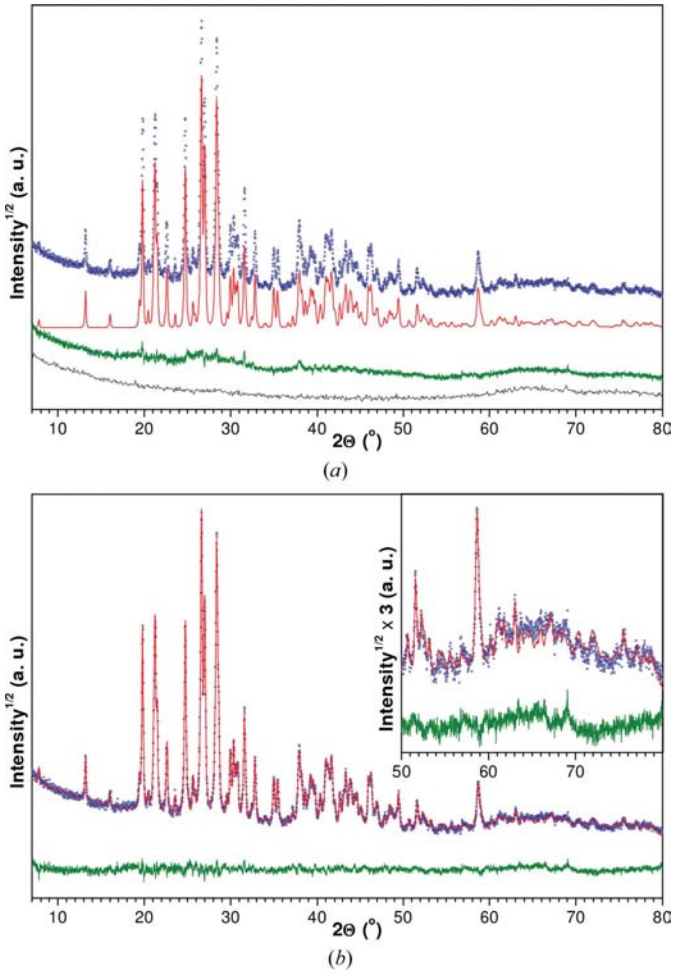

Figure 4
Weighted observed, calculated and difference XRD powder profiles for sample *B* after (*a*) DDM and (*b*) Rietveld refinement. The bottom curve in (*a*) is the sample holder scattering profile.

the conjugate nitroguanidine and the tetrazole molecular fragments. Therefore, despite the overall planarity of the anion it lacks through conjugation.

The coordination of the K^+ cation indicates that the negative charge of the anion is, most probably, delocalized on both the tetrazolyl and the nitroguanyl fragments. Each cation is coordinated by eight atoms from six anions (Fig. 5), five being O atoms and the remaining ones N atoms.

All the H atoms participate in hydrogen bonding. The hydrogen-bond distances and angles are listed in Table 3. N3—H1···O1 and N3—H2···N5 are intramolecular, whilst N4–H3···N8 connects the anions into dimers in the crystal structure (Fig. 6). While the N3—H1···O1 [114 (4)°] angle does not fully satisfy the geometrical criteria of the hydrogen-bond limits, nevertheless, the N3—O1 [2.576 (5) Å] and O1···H1 [2.13 (5) Å] bond lengths are short enough to consider this hydrogen bonding (Zefirov & Zorkii, 1989; Steiner, 2000).

The crystal structure of the potassium salt of TetrNQ determined in this study, with the location of the H atoms, allows its unambiguous assignment to the structural formula (II*a*). This in turn may suggest that the structure of the initial TetrNQ compound may also correspond to the formula type (I*a*) with the classical configuration of the tetrazole fragment. As shown by the structural data obtained, the deprotonation of TetrNQ during the formation of the potassium salt occurs on the N8 atom. As in the case of other nitrimines exhibiting NH acid properties, the initial ionization centre does not coincide with the centre of the negative charge localization (Metelkina *et al.*, 1995; Vasiliev, Astakhov, Nefedov & Stepanov, 2003; Vasiliev, Astachov, Molokeev, Kruglyakova, Sirotinin & Stepanov, 2004; Astachov, Vasiliev, Molokeev, Sirotinin, Kruglyakova & Stepanov, 2004; Astachov, Vasiliev, Molokeev, Kruglyakova, Sirotinin & Stepanov, 2004).

As mentioned above, the quantum-chemically calculated energy for (I*b*) was found to be lower than that for (I*a*) (Astachov *et al.*, 2001; Astachov, Gelemurzina *et al.*, 2003). This disagreement with the structural data obtained is apparently due to the intermolecular interactions in the crystal which were not taken into account in the quantum-chemical calculations carried out for a separate molecule in the gas phase. The intermolecular hydrogen bonds in particular may be responsible for structure (I*a*) being energetically more favourable. The difference in total energy between the optimized conformations (I*a*) and (I*b*) was calculated to be 21.5 kJ mol^{-1} (restricted Hartree–Fock calculation in 6-31G basis), which does not exceed the energy of the strong hydrogen bonds determined for various organic compounds (Domenicano & Hargittai, 1992). The resonance form (II*a*) describes the H-atom location for the crystalline substance and only partly reflects the electron density distribution in the anion. Considering the bond lengths determined and the delocalization of the π-electron density in the nitroguanyl and tetrazolyl fragments, the structure of the TetrNQ anion may be described by the following scheme.

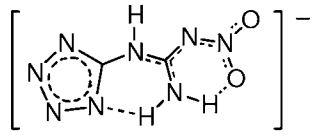

From the structural characteristics available for the potassium salt of TetrNQ and other nitroguanidine derivatives (Nordenson, 1981; Nordenson & Hvoslev, 1981; Rice *et al.*, 1984; Oyumi *et al.*, 1987; Bracuti, 1999; Astachov, Vasiliev, Molokeev, Kruglyakova & Stepanov, 2002; Astachov, Vasiliev, Molokeev, Kekin, Kruglyakova & Stepanov, 2003; Vasiliev *et al.*, 2003*a*,*b*; Vasiliev, Astachov, Molokeev, Kruglyakova & Stepanov, 2004; Allen, 2002), similar delocalizations of the π-electron density in 1-(tetrazol-5-yl)-2-nitroguanidine may be expected, at least for the nitroguanyl molecular fragment.

4. Conclusions

The present study demonstrates the capabilities of the derivative difference minimization method for applications in powder diffraction structure solution and refinement routines. For the title compound potassium 1-(tetrazol-5-yl)-2-nitroguanidine, DDM allowed the successful location and unconstrained refinement of all the atomic positions in the structure, including the positions of the H atoms from ordinary X-ray powder diffraction data. In comparison to the standard Rietveld refinement involving empirical background modelling,

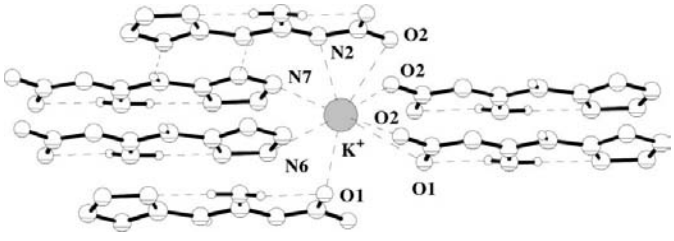

Figure 5
Potassium atom coordination.

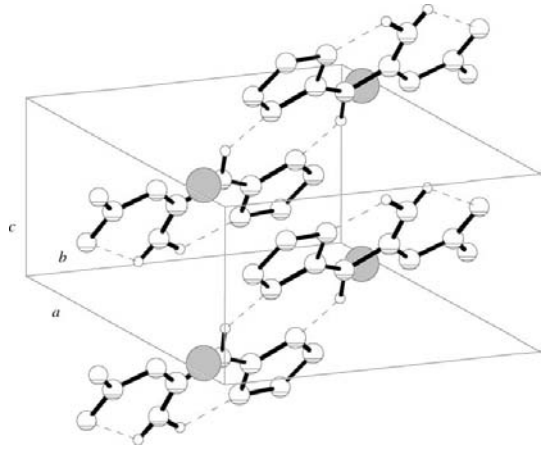

Figure 6
Arrangement of anionic dimers in the potassium 1-(tetrazol-5-yl)-2-nitroguanidine structure. Dashed lines indicate hydrogen bonds.

DDM is shown to provide structural characteristics with higher precision, reproducibility and comprehension. Of course, this example does not establish (and was not aimed at establishing) the absolute impossibility of achieving high-quality structural parameters by Rietveld refinement. Our tests on simulated data have shown that the accuracy of Rietveld refinement is the same as that of DDM if the background is accurately modelled. However, finding an adequate description of the background for real data presents an obvious and generally recognized problem.

While the derivative difference method was primarily designed for cases of complex modulated background, it has also been demonstrated to be advantageous in the common case of a seemingly flat background line. It should be noted that even when the background contribution to a powder pattern is apparently simple, it may have (and normally has) some oscillations which are invisible due to peak overlap. Inadequate background modelling and/or approximations give rise to systematic errors which are avoided in the scheme of DDM. The improvement of the precision provided by the derivative difference method is, evidently, vital for powder diffraction structural analysis as it is a prerequisite for the reliable interpretation of correlations between structure and physico-chemical properties.

This work was partly supported by a Grant-in-Aid for young Russian scientists and the leading scientific schools of the Russian Federation from the Federal Agency on Scientific Innovations.

References

Allen, F. N. (2002). *Acta Cryst.* B**58**, 380–388.

Astachov, A. M., Gelemurzina, I. V., Vasiliev, A. D., Nefedov, A.A., Kruglyakova, L. A. & Stepanov, R. S. (2001). *Energetic Materials – Ignition, Combustion and Detonation.* 32th Int. ICT Conf., Karlsruhe, Germany, 139/1–139/10.

Astachov, A. M., Sokolenko, W. A., Zorin, V. E., Falaleev, O. V., Rubailo, A. I. & Stepanov, R. S. (2002). *Energetic Materials – Synthesis, Production and Application.* 33th Int. ICT Conf., Karlsruhe, Germany, 56/1–56/14.

Astachov, A. M., Vasiliev, A. D., Molokeev, M. S., Kruglyakova, L. A. & Stepanov, R. S. (2002). *New Trends in Research of Energetic Materials.* Proc. V Int. Seminar, Pardubice, Czech Republic, pp. 29–41.

Astachov, A. M., Gelemurzina, I. V., Nefedov, A. A., Kruglyakova, L. A., Vasiliev, A. D., Sokolenko, V. A., Semyannikov, P. P., Trubin, S. V., Dyugaev, K. P., Fedorov, V. A. & Buka, E. S. (2003). *Modern Problems of Technical Chemistry.* Proc. All-Russia Scientific and Technical Conference, Kazan, Russia, pp. 29–40 (in Russian).

Astachov, A. M., Vasiliev, A. D., Molokeev, M. S., Kekin, Yu. V., Kruglyakova, L. A. & Stepanov, R. S. (2003). *J. Struct. Chem.* **44**, 364–368 (in Russian).

Astachov, A. M., Vasiliev, A. D., Molokeev, M. S., Kruglyakova, L. A., Sirotinin, A. M. & Stepanov, R. S. (2004). *J. Struct. Chem.* **45**, 562–565 (in Russian).

Astachov, A. M., Vasiliev, A. D., Molokeev, M. S., Sirotinin, A. M., Kruglyakova, L. A. & Stepanov, R. S. (2004). *J. Struct. Chem.* **45**, 181–186 (in Russian).

Bracuti, A. J. (1999). *J. Chem. Cryst.* **29**, 671–676.

Cernik, R. J., Cheetham, A. K., Prout, C. K., Watkin, D. J., Wilkinson, A. P. & Willis, B. T. M. (1991). *J. Appl. Cryst.* **24**, 222–226.

Dinnebier, R. E., Von Dreele, R., Stephens, P. W., Jelonek, S. & Sieler, J. (1999) *J. Appl. Cryst.* **32**, 761–769.

Domenicano, A. & Hargittai, I. (1992). *Accurate Molecular Structures: Their Determination and Importance.* Oxford University Press. Translated into Russian (1997), Moscow, Mir, pp. 546–547 (in Russian).

Jacob, D. S., Ishay, B., Lavi, R., Solovyov, L. A., Felner, I., Persky, R., Gottlieb, H. E. & Gedanken, A. (2005). *Eur. J. Inorg. Chem.* In the press.

Kim, T.-W., Ryoo, R., Gierszal, K. P., Jaroniec, M., Solovyov, L. A., Sakamoto, Y. & Terasaki, O. (2005). *J. Mater. Chem.* **15**, 1560–1571.

Kleitz, F., Solovyov, L. A., Anilkumar, G. M., Choi, S. H. & Ryoo, R. (2004). *Chem. Commun.* pp. 1536–1537.

Le Bail, A., Duroy, H. & Fourquet, J. L. (1988). *Mater. Res. Bull.* **23**, 447–452.

Leineweber, A., Friedriszik, M. W. & Jacobs, H. (1999). *J. Solid State Chem.* **147**, 229–234.

Metelkina, E. L., Varlygo, K. V. & Paperno, T. Ya. (1995). *Russ. J. General. Chem.* **65**, 1693–1697 (in Russian).

Nordenson, S. (1981). *Acta Cryst.* B**37**, 1543–1547.

Nordenson, S. & Hvoslev, J. (1981). *Acta Cryst.* B**37**, 373–378.

Oyumi, Y., Rheingold, A. L. & Brill, T. B. (1987). *Propellants Explos. Pyrotech.* **12**, 46–52.

Rice, S., Cheng, M. Y., Cramer, R. E., Mandel, M., Mower, H. F. & Seff, K. (1984). *J. Am. Chem. Soc.* **106**, 239–243.

Rietveld, H. (1969). *J. Appl. Cryst.* **2**, 65–71.

Savitzky, A. & Golay, M. J. E. (1964). *Anal. Chem.* **36**, 1627–1639.

Schmidt, M. W., Finger, L. W., Angel, R. J. & Dinnebier, R. E. (1998). *Am. Mineral.* **83**, 881–888.

Schwartz, K. B. & Von Dreele, R. B. (1997) *Adv. X-ray Anal.* **39**, 515–521.

Solovyov, L. A. (2004). *J. Appl. Cryst.* **37**, 743–749 (DDM program is available from http://icct.krasn.ru/eng/content/persons/Sol_LA/ddm.html).

Solovyov, L. A., Belousov, O. V., Dinnebier, R. E., Shmakov, A. N. & Kirik, S. D. (2005). *J. Phys. Chem. B*, **109**, 3233–3237.

Soulie, J.-Ph., Renaudin, G., Cerny, R. & Yvon, K. (2002). *J. Alloys Comput.* **346**, 200–205.

Steiner, T. (2000). *IUCr Newsl.* **8**, No. 4, 19–20.

Vasiliev, A., Astachov, A. & Gelemurzina, I. (2001). Powder Diffraction File #52–2131 of the International Centre for Diffraction Data, Swarthmore, PA.

Vasiliev, A. D., Astachov, A. M., Molokeev, M. S., Kruglyakova, L. A. & Stepanov, R. S. (2003*a*). *Acta Cryst.* E**59**, o193–o194.

Vasiliev, A. D., Astachov, A. M., Molokeev, M. S., Kruglyakova, L. A. & Stepanov, R. S. (2003*b*). *Acta Cryst.* C**59**, o550–o552.

Vasiliev, A. D., Astachov, A. M., Molokeev, M. S., Kruglyakova, L. A. & Stepanov, R. S. (2004). *J. Struct. Chem.* **45**, 558–561 (in Russian).

Vasiliev, A. D., Astakhov, A. M., Nefedov, A. A. & Stepanov, R. S. (2003). *J. Struct. Chem.* **44**, 322–325.

Vasiliev, A. D., Astachov, A. M., Molokeev, M. S., Kruglyakova, L. A., Sirotinin, A. M. & Stepanov, R. S. (2004). *J. Struct. Chem.* **45**, 378–382 (in Russian).

Visser, J. W. (1969). *J. Appl. Cryst.* **2**, 89–95.

Wiles, D. B. & Young, R. A. (1981). *J. Appl. Cryst.* **14**, 149–151.

Zefirov, Yu. V. & Zorkii, P. M. (1989). *Russ. Chem. Rev.* **58**, 713–746 (in Russian).